



POLITECNICO
MILANO 1863

**SCUOLA DI INGEGNERIA INDUSTRIALE
E DELL'INFORMAZIONE**

EXECUTIVE SUMMARY OF THE THESIS

Techno-economic analysis of green ammonia production in innovative Catalytic Membrane Reactor

LAUREA MAGISTRALE IN ENERGY ENGINEERING - INGEGNERIA ENERGETICA

Author: LORENZO PARISI

Advisor: PROF. GIAMPAOLO MANZOLINI

Co-advisor: PROF. FAUSTO GALLUCCI DR. IOLANDA GARGIULO

Academic year: 2023-2024

1. Introduction

Hydrogen is expected to play a key role in achieving EU objectives to reduce greenhouse gas emissions by a minimum of 55% by 2030 and reach net zero emissions by 2050. However, due to its low volumetric density, hydrogen is associated with storage and transportation problems. Ammonia appears to be a potential solution to the challenges with hydrogen. Ammonia can be liquefied by either cooling it below -33°C (at atmospheric pressure) or pressurizing it above 7.5 bar (at 20°C) conditions significantly more attainable than those required for hydrogen liquefaction, which demands cooling below -253°C . Furthermore, liquefied ammonia has an energy density of 12.92/14.4 MJ/L , compared to 8.49 MJ/L for liquid hydrogen (see Table 1) [1]. Developing a method to store renewable hydrogen within ammonia could address many of the challenges associated with hydrogen storage. The Haber-Bosch process, combining hydrogen gas with nitrogen gas to produce ammonia, offers a means to store hydrogen within ammonia. Subsequently, hydrogen can be extracted as needed by heating ammonia to high temperatures. [2]

Table 1: Characteristics comparison of H_2 and NH_3 [1];^aAt 20°C and 10 bar ^bAt -33°C

| Properties | Units | H_2 | NH_3 |
|---------------------------------|-----------------------------|------------------|--------------------------------------|
| phase | [-] | liquid | liquid |
| density | $[\text{kg}/\text{m}^3]$ | 70.8 | 610 ^a /680 ^b |
| boiling point | $[^{\circ}\text{C}]$ | -253 | -33 |
| volumetric H_2 content | $[\text{KgH}_2/\text{m}^3]$ | 70.8 | 107.7/120 |
| volumetric energy density | $[\text{MJ}/\text{L}]$ | 8.49 | 12.92/14.4 |
| H_2 release | [-] | evaporation | cracking ($> 425^{\circ}\text{C}$) |
| flammability/toxicity | [-] | highly flammable | toxic |

A well-established global ammonia infrastructure already exists, with considerable maritime trading of ammonia. International shipping routes are firmly established, and there is a comprehensive network of ports worldwide equipped to handle large-scale ammonia transport. Leveraging this existing port and shipping infrastructure could facilitate the rapid adoption of large-scale ammonia transportation as an energy carrier and fuel. [3]

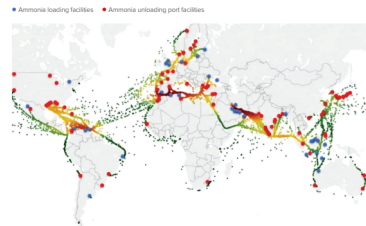
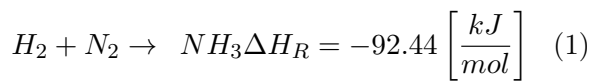


Figure 1: Ammonia shipping infrastructure [3]

In the literature, several studies on the techno-economic analysis of ammonia production can be found. Noshervani et al. compares three methods of ammonia production that differ only in the upstream production of hydrogen and nitrogen, with the synthesis loop being the same for all three. The conventional method using steam reforming results in the lowest cost of produced ammonia at $797 \frac{\$}{ton}$. In contrast, the methods utilizing an alkaline electrolyzer and a PEM electrolyzer, both powered by wind turbines, for hydrogen production result in costs of $917 \frac{\$}{ton}$ and $1317 \frac{\$}{ton}$, respectively [4]. Nayak-Luke et al. reported an LCOA around $1200 \frac{\$}{ton}$ [5]. The main focus of this study is on the ammonia synthesis loop, assuming that hydrogen and nitrogen are produced using a PEM electrolyzer and a PSA (Pressure Swing Adsorption).

1.1. Ammonia synthesis

The synthesis equation of ammonia is shown in Eq. (1)



It is an exothermic reaction, favoured at low temperatures, according to the Le Chatelier's Principle. Similarly, increasing the pressure will favor the formation of more ammonia. The Haber-Bosch process, developed a century ago, accounts for 96% of ammonia production. It operates at pressures ranging from 100 to 300 bar and relies on elevated temperatures, even if this is in contrast with the thermodynamic, typically in the range of 300-500°C.

These conditions, along with specific catalysts, are employed to overcome the activation energy required to break the nitrogen triple bond and accelerate the reaction kinetics. Nitrogen dissociation represents the rate-determining step in the process.

Iron-based catalysts have historically been the primary choice for ammonia synthesis, although ruthenium has gained attention recently for its superior performance. However, its widespread use is hindered by high cost and susceptibility to hydrogen poisoning, which limits ammonia production. In contrast, iron catalysts offer a more economical and durable option.

Ammonia production plants can be divided into two sections: the first involves hydrogen production, while the second relates to the ammonia synthesis loop. In the conventional process, hydrogen is produced through steam reforming. To enhance sustainability, the aim is to employ electrolyzers for hydrogen production and PSA for nitrogen production, thus reducing CO₂ emissions linked to this energy-intensive process. This approach seeks to optimize the utilization of electricity generated by renewable power plants.

The ammonia synthesis loop consists of a compression unit, reactors for ammonia synthesis, an ammonia separation system, a recirculation loop, and a storage unit.

1.2. Catalytic Membrane Reactor

In this study, the conventional reactor series will be replaced by the catalytic membrane reactor (CMR), which is a combination of a heterogeneous catalyst and a perm-selective membrane, which is a thin film layer that allows one component of a mixture to selectively permeate through it. Membrane processes are characterized by the fact that the feed stream is divided into 2 streams: retentate and permeate. The retentate is that part of the feed that does not pass through the membrane, while the permeate is that part of the feed that does pass through the membrane. The optional "sweep" is a gas that is used to help remove the permeate. The CMR operates in the following manner: the retentate, housing the catalyst, in pellet form, to facilitate ammonia synthesis, is delineated from the permeate by a carbon membrane, fortified by ceramic support to endure the elevated temperatures inherent to the process. The ammonia synthesis reaction occurs only in the retentate and the NH_3 produced diffuse through the membrane. Simultaneously, external to the retentate, the sweep gas, flowing congruently with the feed, aids in permeate extraction while enhancing heat transfer between retentate and permeate. (Fig. 3)

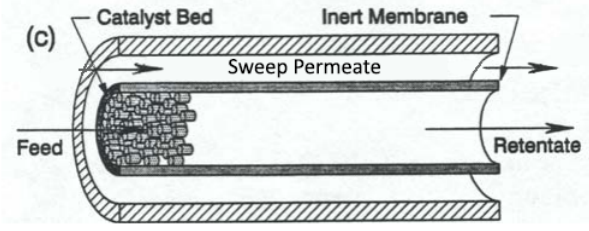


Figure 2: Architecture of the Catalytic Membrane Reactor

The main mechanism of gas transport through membranes are: Knudsen diffusion, viscous flow, selective adsorption and surface diffusion and molecular sieving. The latter will be the one exploited by the carbon membrane adopted in this study.

2. Method

The analysis is divided into two levels: the first concerns the reactor model, while the second pertains to the plant analysis, which was performed using Aspen Plus, followed by the economic analysis.

The reactor model has been developed using MATLAB. The dimension where reactants and products flow is the axial one. Subsequently, the MATLAB model is called by Aspen Plus, a process simulation software used in the chemical and associated industries for modeling, designing, and optimizing chemical processes, to simulate the entire process. The kinetic adopted for a commercially available ammonia synthesis Fe catalyst is represented in Eq. (2) [6]:

$$r_{N_2} = 2k \left[K_{eq}^2 \cdot a_{N_2} \left(\frac{a_{H_2}^3}{a_{NH_3}^2} \right)^\alpha - \left(\frac{a_{NH_3}^2}{a_{H_2}^3} \right)^{1-\alpha} \right] \quad (2)$$

The kinetic adopted for the Ruthenium catalyst is represented in Eq. (3) [7]

$$r_{N_2} = k \cdot \lambda \cdot \frac{a_{N_2}^{0.5} \left[\frac{a_{H_2}^{0.375}}{a_{NH_3}^{0.25}} \right] - \frac{1}{K_{eq}} \left[\frac{a_{NH_3}^{0.75}}{a_{H_2}^{1.125}} \right]}{1 + K_{H_2} a_{H_2}^{0.3} + K_{NH_3} a_{NH_3}^{0.2}} \quad (3)$$

The activities are determined by the fugacity of each component:

$$a_i = f_i = \phi_i \cdot y_i \cdot P \quad (4)$$

To calculate the equilibrium constant it has been

used the equation of Gillespie and Bettie (1930):

$$\log_{10}(K_{eq}) = -2.691122 \cdot \log_{10} T - 5.519265 \cdot 10^{-5} T + 1.848863 \cdot 10^{-7} + T^2 + \frac{2001.6}{T} + 2.6899 \quad (5)$$

The equation of reverse ammonia synthesis reaction has been considered in base of Arrhenius format:

$$k = k_0 \cdot \exp \left(\frac{-E}{R \cdot T} \right) \quad (6)$$

Where :

- $k_{Fe} = 8.849 \cdot 10^{14}$ pre-exponential factor
- $E_{Fe} = 40765$ Activation energy
- $k_{Ru} = 9.02 \cdot 10^8$ pre-exponential factor
- $E_{Ru} = 23000$ Activation energy
- $R = 1.987 \left[\frac{cal}{mol \cdot K} \right]$ Universal gas constant
- T is the Temperature in degrees Kelvin

The two kinetics were validated according to these two studies: the one concerning the iron catalyst was validated based on Nielsen's work [8], while the one concerning the ruthenium catalyst was validated based on Rossetti's research [7].

The assumption regarding the reactor model simulated on Matlab are:

- 1D model
- Peng-Robinson thermodynamic model
- Negligible pressure drop
- Real gas behaviour
- $\frac{L}{D} = 3$

The model solves a system of ODEs and takes as inputs the molar flow rates of each component, the temperatures of the retentate and permeate, the pressures, and the input data characterizing the reactor and the membrane (see Table 2-3). For each integration step, it calculates the partial pressures of each component and the reaction rate according to Eq. 2 and 3. It also determines the flux of each component through the membrane based on Eq 8, ensuring mass and energy balances described in Eq.(9-12).

The conversion χ_{N_2} was analyzed at various values of gas hourly space velocity (GHSV) defined as in Eq.7 because the reaction occurs only in the retentate.

$$GHSV = \frac{F_{in,ret}}{V_{tot} \cdot (1 - \epsilon)} \left[\frac{1}{h} \right] \quad (7)$$

In Table 2 are shown the parameters chosen to characterize a catalytic reactor, which include:

the diameter of the catalyst particle d_p , the catalyst particle density ρ_c , the catalyst dilution factor D_{cat} and the bed voidage ϵ .

Table 2: Catalyst bed parameters

| Parameter | Value | Unit |
|--------------|---------------------|------------------|
| d_p | $2.5 \cdot 10^{-3}$ | m |
| D_{cat} | $\frac{1}{3}$ | $[-]$ |
| ρ_{cFe} | 2800 | $\frac{kg}{m^3}$ |
| ρ_{cRu} | 590 | $\frac{kg}{m^3}$ |
| ϵ | 0.4 | $[-]$ |

Table 3 presents key data used to characterize the membrane: D_m^o and D_m^i are the external and the internal diameter of the membrane, σ_{NH_3/H_2} and σ_{NH_3/N_2} the ammonia selectivity concerning both hydrogen and nitrogen, \mathcal{P}_{NH_3} the ammonia permeability and $Sweep_{gas}$ is the required amount of sweep gas, defined in this instance as the molar inflow rate into the retentate.

Table 3: Membrane reactor parameters

| Parameter | Value | Unit |
|----------------------|--------------------|---------------------|
| D_m^o | $10 \cdot 10^{-3}$ | m |
| D_m^i | $7 \cdot 10^{-3}$ | m |
| \mathcal{P}_{NH_3} | $4 \cdot 10^{-7}$ | $[-]$ |
| σ_{NH_3/H_2} | 50 | $[-]$ |
| σ_{NH_3/N_2} | 1000 | $[-]$ |
| $Sweep_{gas}$ | F_{inret} | $[\frac{kmol}{hr}]$ |

J_i is the flux of the component i passing through the membrane, which is calculated according to Eq. (7). It is considered to be positive when the flow is going from retentate to permeate.

$$J_i = \mathcal{P}_i \cdot (P_i^R - P_i^P) \quad (8)$$

\mathcal{P}_i $[\frac{mol}{Pa \cdot s \cdot m^2}]$ accounts for the permeance of each gas, while P_i^R and P_i^P accounts for the partial pressure of each gas of the retentate and permeate side.

The mass balance for both retentate and permeate side are presented in this section. For each component we have the following equations:

$$\frac{dF_i^R}{dL} = \theta_i \cdot r_i \cdot \rho_c \cdot (1 - \epsilon) \cdot \frac{\pi}{4} \cdot (D_r^2 - D_m^o{}^2) - J_i \cdot (\pi \cdot D_m^o) \quad (9)$$

$$\frac{dF_i^P}{dL} = J_i \cdot (\pi \cdot D_m^o) \quad (10)$$

Where θ_i is the stoichiometric coefficient, r_i is the reaction rate, ρ_c is the catalyst density. D_r is the diameter of the reactor.

Likewise the mass balance, the energy balance equations are computed for the retentate and the permeate side.

$$\frac{dT^R}{dL} = \frac{r \cdot (-\Delta H_R) \cdot \rho_c \cdot (1 - \epsilon) \cdot \frac{\pi}{4} \cdot (D_r^2 - D_m^o{}^2)}{\sum_i F_i^R \cdot cp_i^R} + \frac{U \cdot N_m \cdot \pi \cdot D_m^i \cdot (T^R - T^P)}{\sum_i F_i^R \cdot cp_i^R} \quad (11)$$

$$\frac{dT^P}{dL} = \frac{U \cdot N_m \cdot \pi \cdot D_m^i \cdot (T^R - T^P)}{\sum_i F_i^P \cdot cp_i^P} \quad (12)$$

Where N_m is the number of the membrane adopted inside the reactor and U is the global heat transfer coefficient, which describes three heat transfer phenomena:

1. The convection in the inner tube
2. The conduction through the membrane
3. The convection in the outer tube

$$U = \left[\frac{1}{h^P} + \frac{\frac{D_m^i}{2} \cdot 2 \cdot \ln \frac{D_r}{D_m^i}}{k} + \frac{D_m^i}{D_r} \cdot \frac{1}{h^R} \right]^{-1} \quad (13)$$

The heat transfer coefficient in the reaction zone, h^R , has been calculated according to the correlation of Li and Finalyson [9], which takes in account the heat transfer of a packed bed by referring to a Reynold's number depending on particle diameter. As for permeate zone, h^P , has been calculated according to the correlation of Dittus-Boelter which consider a smooth concentric anulus [10]. Lastly the conductivity, which is referred in this case to a carbon membrane, has been calculated as contribution of the carbon layer thermal conductivity and $\alpha - Al_2O_3$ (the membrane support) thermal conductivity through a correlation [11]. Thermodynamic properties like density, viscosity, specific heat and thermal conductivity are determined using correlations. [12–15].

Aspen Plus was used to simulate the ammonia synthesis loop with both the conventional reactor and the membrane reactor. The main assumption adopted in Aspen Plus are:

- Math Model \rightarrow Peng-Robinson EoS

- Steady-State Model
- Target Output = 100 $\frac{\text{ton}_{NH_3}}{\text{day}}$
- NH_3 purity > 99.9%
- GHSV = 1000

Table 4: Aspen assumptions

| Parameter | Value | Unit |
|------------------|-------|-------------------|
| Δp | 0 | bar |
| ΔT_{app} | 10 | $^{\circ}C$ |
| η_{iso} | 87 | % |
| η_{mecc} | 95 | % |
| T_{cond} | -85 | $^{\circ}C$ |
| U_{HX} | 0.02 | $\frac{kW}{m^2K}$ |

The conventional ammonia synthesis loop includes three reactors arranged in series to address thermodynamic and kinetic limitations. After each reactor, the gas is cooled to improve overall conversion. In contrast, the loop with a membrane reactor requires only a single reactor. Subsequently, the ammonia-rich gas is cooled and separated through condensation, while the unconverted reactants are recirculated. The layout of the two plants are shown in Figure 3 and Figure 4.

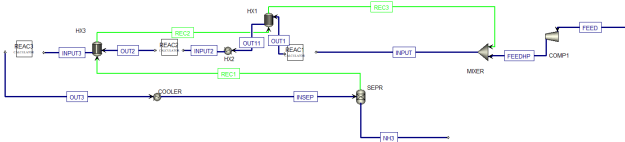


Figure 3: Layout of the plant adopting the conventional reactors

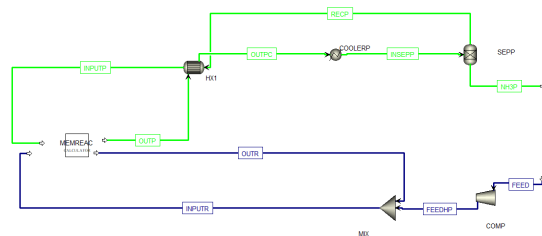


Figure 4: Layout of the plant adopting the membrane reactor

The primary Key Performance Indicator (KPI) for assessing the superiority of the membrane reactor plant over the conventional one is the COP (production cost of ammonia produced).

The economic analysis was conducted using the NETL (National Energy Technology Laboratory) approach [16].

From the cost of each equipment is calculated the BEC (Bare Erected Cost). Eq. 14 describe how the cost of each component has been calculated. Q_b is a capacity in terms of the scaling parameter of the known base reference, M is a constant depending on the equipment type, f_p, f_t and f_m are indexes that account for the material of construction, the pressure and the temperature. The CEPCI (Chemical Engineering Plant Cost Index) is a tool for chemical process industry to compare plant construction from one period to another.

$$C_E = \frac{CEPCI_{2023}}{CEPCI_{ref}} \cdot \left(\frac{Q}{Q_b}\right)^M \cdot f_p \cdot f_t \cdot f_m \quad (14)$$

Once the BEC has been calculated, it is then possible to compute the TOC (Total Overnight Costs) as follow in Table 5.

Table 5: Methodology for the calculation of TOC [17]

| Index | Cost (M€) |
|---|------------|
| Total Installation Cost (TIC) | 80% BEC |
| Total Direct Plant Cost (TDPC) | BEC + TIC |
| Indirect Costs (IC) | 14% TDPC |
| Engineering Procurement and Construction (EPC) | TDPC + IC |
| <i>Contingency and Owner's Costs (C&OC)</i> | |
| Contingency | 10% EPC |
| Owner's Cost | 5% EPC |
| Total Overnight Costs (TOC) | EPC + C&OC |

In the end, the CAPEX is annually discounted using the Capital Cost Recovery Factor.

The parameters for the calculation of the Capital Cost recovery Factor are:

- $i = 8\%$, discount rate [18]
- $n = 20$ years, the lifetime of the plant

$$CCF = \frac{i \cdot (1 + i)^n}{(1 - i)^n - 1} \quad (15)$$

$$CAPEX_{yearly} = TOC \cdot CCF \quad (16)$$

On the other hand, OPEX takes into account feedstock, utilities, operations and maintenance (O&M), as well as the catalyst and membranes utilized.

The $OPEX_{feedstock}$ represents the expenses sustained in supplying the hydrogen and the nitrogen, excluding the transportation cost

due to the specific location of the plant. The $OPEX_{utilities}$ is the cost associated to the refrigerants, the cooling water and the electricity to supply the pumps and the compressors. The $OPEX_{O\&M}$ accounts for labor, maintenance and insurance costs and the $OPEX_{variables}$ are the cost associated with catalyst and membranes.

The operating expenses related to the various streams were calculated using Eq. 17.

$$OPEX_i \left[\frac{M\text{€}}{y} \right] = C_i \cdot \dot{m}_i \cdot h_{avail} \cdot 10^{-6} \quad (17)$$

Where the parameters adopted are listed below:

- C_i is the specific cost of the i variable
- \dot{m}_i is the flow rate of the i variable
- h_{avail} represents the annual operating hours assumed for the plant. In this instance, a value of 7884 hours has been selected, equivalent to 90% of the total hours in a year.

The OPEX related to the membrane and the catalyst cost are described in Eq. 18 and Eq. 19, where A_m represent the membrane area utilized and Kg_{cat} the quantity of iron catalyst inside the reactor.

$$OPEX_{membrane} = C_{mem} \cdot Mem_{lifetime} \cdot A_m \quad (18)$$

$$OPEX_{catalyst} = C_{cat} \cdot Cat_{lifetime} \cdot Kg_{cat} \quad (19)$$

All the assumption adopted for the OPEX calculation are listed in Table 6.

Table 6: Assumptions for the calculation of the OPEX

| Index | Unit | Cost (M€) |
|-----------------|------------------------|-------------|
| H_2 | $\frac{\text{€}}{kg}$ | 5.905 |
| N_2 | $\frac{\text{€}}{m^3}$ | 0.250 |
| $Fe_{catalyst}$ | $\frac{\text{€}}{kg}$ | 0.1607 [19] |
| Membrane | $\frac{\text{€}}{m^2}$ | 93 [20] |
| Electricity | $\frac{\text{€}}{kWh}$ | 0.085 |
| Cooling Water | $\frac{\text{€}}{ton}$ | 0.013 |
| Labor | %TOC | 1 |
| Maintenance | %TOC | 2.5 |
| Insurance | %TOC | 2 |

In the end, the production cost of ammonia can be calculated as described in Eq. 20.

$$COP = \frac{OPEX + CAPEX_{yearly}}{\text{ton}_{NH_3 \text{ yearly}}} \left[\frac{\text{€}}{\text{ton}_{NH_3}} \right] \quad (20)$$

3. Analysis

In this section, the most significant analysis leading to the selection of the final configuration for both the conventional reactor and the membrane one will be presented.

These simulations were conducted using a constant molar inlet flow rate of 100 kmol/hr, adopting a $\frac{H_2}{N_2}$ ratio equal to 3, while varying the volume. The pressure is set at 200 bar, the range of inlet temperatures investigated for the feed entering the retentate spans from 370°C to 495°C, as this is the range in which the iron catalyst is active [8], while for the ruthenium catalyst the inlet temperatures spans from 320 °C to 480°C [7]. The pressure drops were neglected for simplicity.

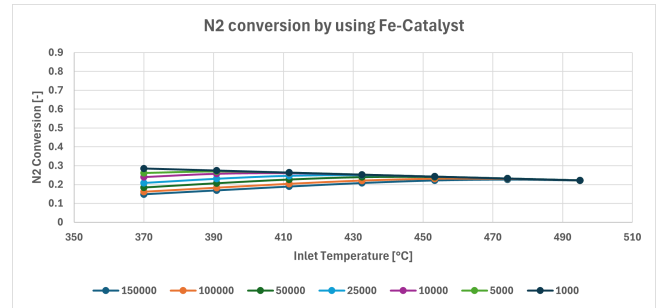


Figure 5: Conversion of the Conventional Reactor varying the inlet temperature with Fe catalyst

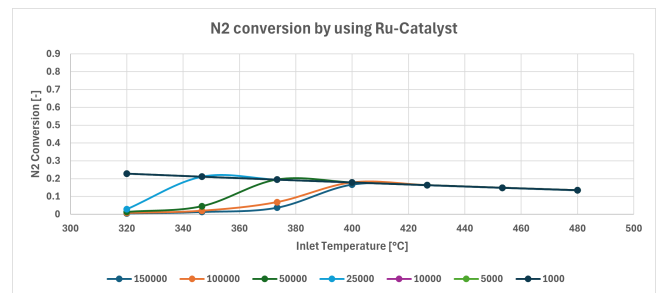


Figure 6: Conversion of the Conventional Reactor varying the inlet temperature with Ru catalyst

These two graphs shows that at low GHSV, both kinetics reach a plateau, and the one using Fe-catalyst exhibits higher conversion (@GHSV = 1000 → 28.49% vs 22.82%). For this reason, it was decided to proceed with the iron catalyst.

For the membrane reactor a membrane area of 10 m^2 was adopted, with the retentate pressure fixed at 200 bar and the permeate pressure at 30 bar¹. The latter was assumed because it was hypothesized that the hydrogen originates from a PEM electrolyzer operating at 30 bar.

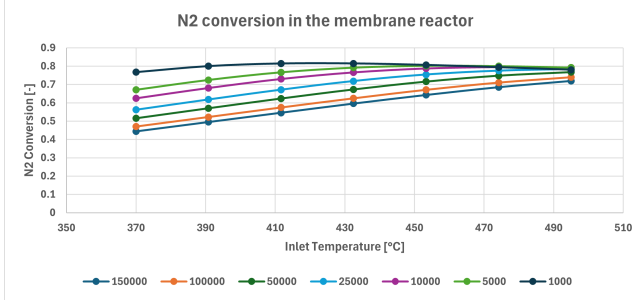


Figure 7: Conversion of the Membrane Reactor varying the inlet temperature

In the membrane reactor, decreasing the space velocity (achieved in this case by increasing the volume) results in higher conversion rates. This occurs due to a decrease in residence time and also because, with an increased volume and a fixed membrane area, the impact of the membrane intensifies. The temperature maximum associated with conversion shifts to the right.

3.1. Effect of the Sweep gas

The function of the sweep gas is to facilitate the extraction of the permeate and improve the heat exchange within the reactor. Since we are able to separate almost 100% of the produced ammonia in the retentate, by increasing the area of the membrane, reducing the amount of sweep gas produced can bring many benefits to the plant. Given the utilization of a porous membrane and the possibility of back permeation, the sweep gas is composed of the same reactants as the feed to prevent contamination of the retentate with additional gases. In the tables below, it can be observed how the quantity and temperature of the sweep affect the reactor dimensions, outlet temperatures, and inlet flow rate required to achieve an output of 100 tons of ammonia.

¹PEM electrolyzer, <https://nelhydrogen.com/product/m-series-electrolyser/>

Table 7: Parameters of the membrane reactor varying the amount of sweep gas

| Property | Sweep = 2 | Sweep = 1.5 | Sweep = 1 |
|-----------------------------|-----------|-------------|-----------|
| $T_{out_{RET}}$ [°C] | 412.55 | 480.56 | 644.49 |
| N_2 Conversion [-] | 0.957 | 0.945 | 0.908 |
| NH_3 Recovery [-] | 0.9994 | 0.9990 | 0.9945 |
| V_{tot} [m ³] | 31.69 | 32.11 | 33.38 |
| FlowRate $\frac{ton}{day}$ | 104.47 | 105.85 | 110.04 |

Table 8: Parameters of the membrane reactor varying the temperature of sweep gas

| Property | T = 370 °C | T = 300 °C | T = 200 °C | T = 80 °C |
|-----------------------------|------------|------------|------------|-----------|
| $T_{out_{RET}}$ [°C] | 701.15 | 691.92 | 681.59 | 644.69 |
| N_2 Conversion [-] | 0.633 | 0.695 | 0.795 | 0.908 |
| NH_3 Recovery [-] | 0.915 | 0.937 | 0.967 | 0.994 |
| V_{tot} [m ³] | 47.94 | 43.68 | 38.16 | 33.38 |
| FlowRate $\frac{ton}{day}$ | 158.04 | 143.83 | 125.8 | 110.04 |

3.2. Effect of the Membrane Area

In Figure 6, it can be observed that increasing the membrane area inside the reactor leads to a conversion plateau for each space velocity. The ammonia recovery reaches its maximum for high membrane area values at low space velocity, indicating that all ammonia produced in the retentate manages to diffuse into the permeate, and the reaction is less limited by thermodynamics.

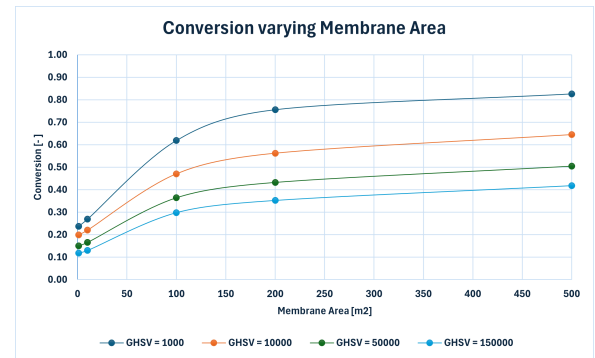


Figure 8: Conversion by varying the membrane area at different GHSV

4. Results

The set objective for this technical-economic analysis is to achieve a production of 100 tons of ammonia per day. The goal is to minimize the cost of the ammonia produced.

The traditional loop for ammonia synthesis incorporates three reactors arranged in series. The feed mixture of hydrogen and nitrogen is pres-

surized to the operating pressure by a centrifugal compressor. An inlet temperature of 370°C is selected for each reactor based on Figure 5, which maximizes the conversion. To overcome thermodynamic and kinetic constraints, the gas exiting each reactor must be cooled to enhance overall conversion. The ammonia produced at the end of the three reactors is cooled to a low temperature of -85°C. The unreacted gas is recycled back for reconversion and also helps cool the hot stream exiting the reactors. However, it is necessary to use a refrigerant for the flow rate entering the second reactor.

In the figure below it can be observed the temperatures and the molar fraction of ammonia exiting each reactor. To maintain the same GHSV, considering that the reaction leads to a decrease in moles, the volumes of the second and third reactors will progressively decrease. Furthermore, the conversion rate will also decrease due to the formation of ammonia. The overall conversion with respect to the N_2 entering the first reactor and the N_2 exiting the third one is equal to 53%.

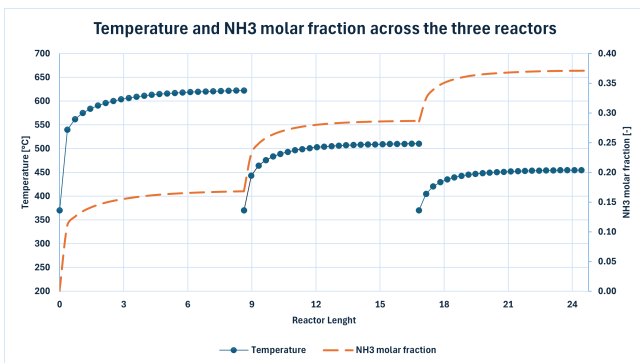


Figure 9: NH_3 molar fraction and temperature of the feed across the reactors

The loop of ammonia synthesis with the membrane reactor is shown in Figure 8. The difference from the conventional setup is the adoption of only one reactor and one heat exchanger. The majority of the ammonia resides in the permeate, so the separation will only occur for this stream. The hot permeate, at the temperature of 586°C, exiting the reactor allows to heat up the retentate to 370 °C and also to warm the cold gases from the separator, which exit at -85°C, to 80°C.

In the very initial moments when the feed is introduced into the reactor, a significant leap in conversion can be observed from the figure be-

low. This implies that the reaction rate is very high. After this jump, the conversion is increasing, which can be linked to the effect of the membrane capable of removing the produced ammonia, thus reducing its partial pressure in the retentate and favoring the formation of more ammonia. In the final stages, since the reaction grows slower in the retentate, the temperature of the two different sections are able to equilibrate.

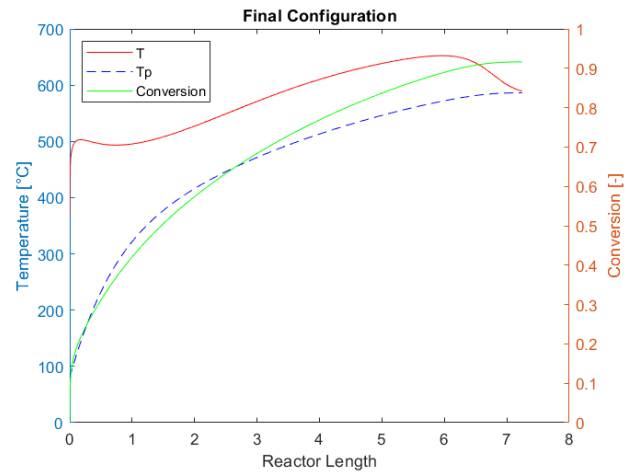


Figure 10: Temperature and Conversion inside the reactor

In the graphs below, it can be observed that the cost of reactors in the conventional plant is significantly higher than that of the membrane plant. This is attributed to lower conversion and larger volumes required.

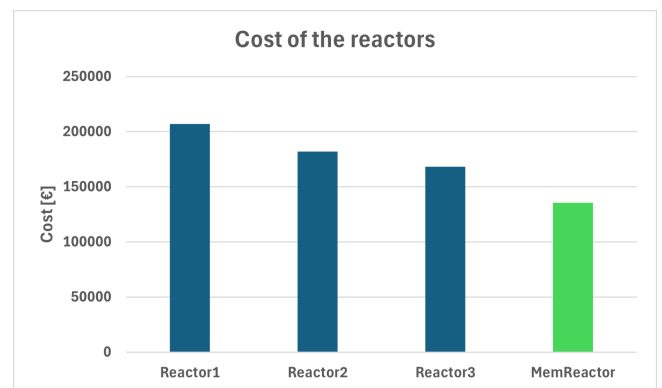


Figure 11: Comparison of reactor's costs

In terms of total equipment costs, those associated with the conventional plant exceed 3.7 million euros. The compressor cost is the most significant factor in both plants.

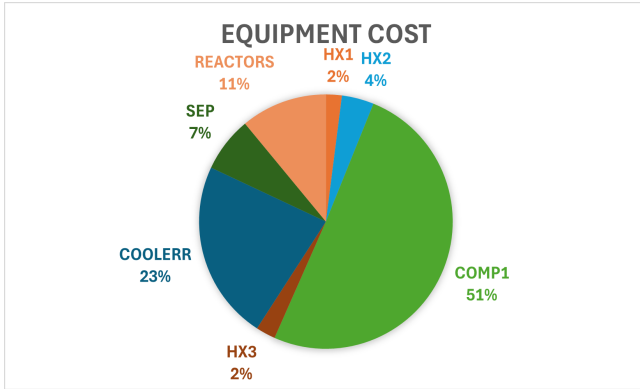


Figure 12: Equipment Costs Conventional Plant

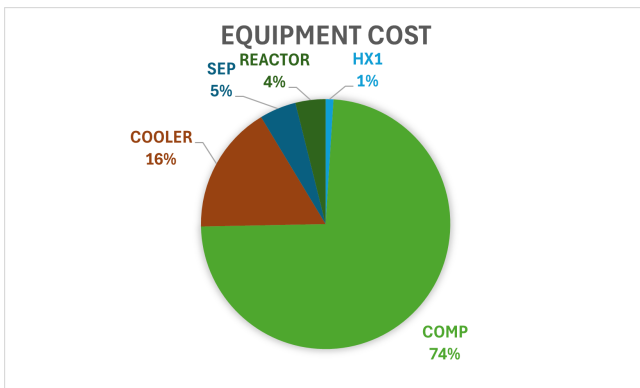


Figure 13: Equipment Costs Membrane Plant

The OPEX of the conventional plant are almost equal to those of the membrane one. The cost that has the most impact is certainly the hydrogen fed into the plant. Considering that the Haber-Bosch process use a recirculation of unreacted products to maximize conversion, the differences in conversion rates observed previously (91% for the membrane reactor and 53% for the conventional reactor series), result in the same amount of feed entering the reactors.

| Index | Conventional | Membrane | Unit |
|------------|--------------|----------|------|
| Utilities | 0.948 | 0.912 | [M€] |
| Feed-stock | 34.479 | 34.479 | [M€] |
| Fixed | 0.658 | 0.424 | [M€] |
| Total | 36.086 | 35.816 | [M€] |

Table 9: OPEX comparison

The final cost of produced ammonia is lower in the plant using the membrane reactor by 21 euros per ton $1136 \frac{\text{€}}{\text{ton}_{NH_3}}$ vs $1117 \frac{\text{€}}{\text{ton}_{NH_3}}$). Comparing these results with those from other studies reveals that these values fall within the expected ranges when PEM electrolyzers are used,

but they are significantly different from those produced by conventional hydrogen production methods, such as steam reforming. However, these comparisons are limited by the differing approaches and hypotheses employed.

5. Conclusion

The primary objective of this study has been to design and conduct a techno-economic evaluation of an ammonia synthesis loop. Specifically, it focuses on comparing two scenarios: one featuring a conventional reactor and the other employing a membrane reactor.

Focusing on single-pass conversion, the membrane reactor configuration proves highly advantageous compared to the conventional one. It allows for a single reactor and smaller volumes to achieve the same output. This advantage isn't evident when recirculation is employed within the Haber process. The potential benefit of employing a membrane reactor over a series of reactors lies in utilizing fewer components within the plant. Furthermore, ongoing research into new catalysts capable of facilitating the process at lower temperatures and pressures is underway. These catalysts could work with hydrogen to nitrogen ratios below 3. Since a significant portion of ammonia production costs are attributed to hydrogen, substantial cost reductions may be realized. Also adopting a different separation mechanism from the conventional one might result in lower capital expenses and consequently affect the overall cost of production.

References

- [1] Limitations of Ammonia as a Hydrogen Energy Carrier for the Transportation Sector | ACS Energy Letters.
- [2] Oscar Serpell. Ammonia's Role in a Net-zero Hydrogen Economy.
- [3] The Royal Society. Ammonia: zero-carbon fertiliser, fuel and energy store.
- [4] Shahmir Ali Noshervani and Rui Costa Neto. Techno-economic assessment of commercial ammonia synthesis methods in coastal areas of Germany. *Journal of Energy Storage*, 34:102201, February 2021.
- [5] Richard Nayak-Luke, René Bañares-Alcántara, and Ian Wilkinson. "Green"

- Ammonia: Impact of Renewable Energy Intermittency on Plant Sizing and Levelized Cost of Ammonia. *Industrial & Engineering Chemistry Research*, 57(43):14607–14616, October 2018.
- [6] D. C. Dyson and J. M. Simon. Kinetic Expression with Diffusion Correction for Ammonia Synthesis on Industrial Catalyst. *Industrial & Engineering Chemistry Fundamentals*, 7(4):605–610, November 1968.
- [7] Ilenia Rossetti, Nicola Pernicone, Francesco Ferrero, and Lucio Forni. Kinetic Study of Ammonia Synthesis on a Promoted Ru/C Catalyst. *Industrial & Engineering Chemistry Research*, 45(12):4150–4155, June 2006. Publisher: American Chemical Society.
- [8] Anders Nielsen, Jørgen Kjaer, and Bennie Hansen. Rate equation and mechanism of ammonia synthesis at industrial conditions. *Journal of Catalysis*, 3(1):68–79, February 1964.
- [9] Shriniwas S. Chauk and Liang-Shih Fan. HEAT TRANSFER IN PACKED AND FLUIDIZED BEDS. In Warren M. Rohsenow, James P. Hartnett, and Young I. Cho, editors, *Handbook of Heat Transfer*. McGraw-Hill Education, 1st edition edition, 1998.
- [10] J. Dirker and Josua Meyer. Convective Heat Transfer Coefficients in Concentric Annuli. *Heat Transfer Engineering - HEAT TRANSFER ENG*, 26:38–44, March 2005.
- [11] Serena Poto, Fausto Gallucci, and M. Fernanda Neira d’Angelo. Direct conversion of CO₂ to dimethyl ether in a fixed bed membrane reactor: Influence of membrane properties and process conditions. *Fuel*, 302:121080, October 2021.
- [12] Juan Sebastian Lopez-Echeverry, Simon Reif-Acherman, and Eduard Araujo-Lopez. Peng-Robinson equation of state: 40 years through cubics. *Fluid Phase Equilibria*, 447:39–71, September 2017.
- [13] Jean-Noël Jaubert and Fabrice Mutelet. VLE predictions with the Peng–Robinson equation of state and temperature dependent k_{ij} calculated through a group contribution method. *Fluid Phase Equilibria*, 224(2):285–304, October 2004.
- [14] Don W Green and Marylee Z Southard. Perry’s Chemical Engineers’ Handbook (9780071834094).
- [15] J. Richard Elliott, Vladimir Diky, Thomas A. Knotts, and W. Vincent Wilding. *Properties of Gases and Liquids*. McGraw-Hill Education, 6th edition edition, 2023.
- [16] Kristin Gerdes, William Summers, and John Wimer. Quality Guidelines for Energy System Studies: Cost Estimation Methodology for NETL Assessments of Power Plant Performance. Technical Report DOE/NETL-2011/1455, 1513278, August 2011.
- [17] G. Manzolini, E. Sanchez Fernandez, S. Rezvani, E. Macchi, E.L.V. Goetheer, and T.J.H. Vlught. Economic assessment of novel amine based CO₂ capture technologies integrated in power plants based on European Benchmarking Task Force methodology. *Applied Energy*, 138:546–558, January 2015.
- [18] Carlos Arnaiz Del Pozo and Schalk Cloete. Techno-economic assessment of blue and green ammonia as energy carriers in a low-carbon future. *Energy Conversion and Management*, 255:115312, March 2022.
- [19] Yaroslav Grosu, Abdessamad Faik, Iñigo Ortega-Fernández, and Bruno D’Aguanno. Natural Magnetite for thermal energy storage: Excellent thermophysical properties, reversible latent heat transition and controlled thermal conductivity. *Solar Energy Materials and Solar Cells*, 161:170–176, March 2017.
- [20] Danlin Chen, Feng Yang, Dionysis S. Karousos, Linfeng Lei, Evangelos P. Favvas, and Xuezhong He. Process parametric testing and simulation of carbon membranes for H₂ recovery from natural gas pipeline networks. *Separation and Purification Technology*, 307:122842, February 2023.